Nuclear Instruments and Methods in Physics Research A 444 (2000) 151–155

NUCLEAR INSTRUMENTS & METHODS IN PHYSICS RESEARCH Section A

www.elsevier.nl/locate/nima

Fiske modes in superconducting tunnel junction detectors

S. Friedrich[a,b,*], M.F. Cunningham[a], M. Frank[a], S.E. Labov[a], A.T. Barfknecht[c], S.P. Cramer[b]

[a]Lawrence Livermore National Laboratory, P.O. Box 808, L-418, Livermore, CA 94550, USA
[b]Lawrence Berkeley National Laboratory, MS 6-2100, Berkeley, CA 94720, USA
[c]Conductus Inc., 969 West Maude Ave., Sunnyvale, CA 94086, USA

Abstract

We are developing superconducting tunnel junction (STJ) X-ray spectrometers with high-energy resolution (< 10 eV for keV X-rays) and high count rate capabilities (> 10 000 counts/s). We have examined the influence of Fiske mode resonances on energy resolution, maximum count rate and area of Nb–Al–AlOx–Al–Nb STJ detectors. At low count rate, these detectors have an energy resolution of 2.3 eV FWHM at 70 eV. At 20 000 counts/s, the resolution is 8.2 eV FWHM at 277 eV. We observe the optimum detector performance when the influence of Fiske modes is minimized. © 2000 Published by Elsevier Science B.V. All rights reserved.

Keywords: Cryogenic X-ray detectors; Superconducting tunnel junctions; Fiske modes

1. Introduction

X-ray detectors can be characterized by their energy resolution, maximum count rate and their efficiency over an effective area. In recent years, there has been an increasing interest in X-ray detectors operated at temperatures below 1 K, primarily because they offer energy resolution below 10 eV for X-ray energies up to 10 keV [1,2]. The development of these detectors was initially driven by X-ray and particle astrophysics [3,4]. More recently, applications in microanalysis [5], material science [6] and biophysics [7,8] have emerged and are being pursued for scientific and commercial interest. For each of these applications, the relative importance of resolution, count rate and efficiency times effective area is different.

Cryogenic X-ray detectors fall into two main groups: microcalorimeters and superconducting tunnel junctions (STJs). Microcalorimeters measure the X-ray induced temperature rise of a sensitive thermistor, typically a doped semiconductor [4,9] or a superconducting transition edge sensor [5]. Microcalorimeters have demonstrated excellent energy resolution below 8 eV FWHM at 6 keV [4,5,9,10]. This resolution comes at the expense of a lower maximum count rate (around 500 counts/s), because the relaxation of thermal devices back to their equilibrium is intrinsically slow [5]. STJ detectors measure the excess tunneling current produced when an X-ray is absorbed in one of the junction electrodes and generates excess free charge carriers called quasiparticles. STJ detectors have achieved a resolution between 12 and 15.7 eV

*Correspondence address: Lawrence Livermore National Laboratory, P.O. Box 808, L-418, Livermore, CA 94550, USA.
E-mail address: friedrich1@llnl.gov (S. Friedrich).

0168-9002/00/$ - see front matter © 2000 Published by Elsevier Science B.V. All rights reserved.
PII: S0168-9002(99)01348-0

FWHM at 6 keV [11,12] and between 4.6 and 8.9 eV for 0.2 to 1 keV photons [13]. However, they can be operated at significantly higher count rates of order 10 000 counts/s [14]. A common challenge with cryogenic X-ray detectors is their small effective area, typically of order $200\times200\ \mu m^2$.

One unavoidable disturbance in large STJ detectors are Fiske mode resonances [15], which occur whenever the AC Josephson current excites a cavity mode in the insulating tunneling barrier region between the junction electrodes. Fiske modes manifest themselves as resonance peaks in the $I(V)$ characteristics of the STJ detector. In square junctions with a magnetic field applied in the plane of the junction parallel to the junction sides, the resonance condition is satisfied when the junction width is an integral multiple of half the wavelength of the AC Josephson radiation ($f = 486$ MHz/μV) [16]. In shaped junctions, or in cases when the magnetic field is not parallel to the junction sides, the Fiske mode positions are more complicated to calculate. Still, the dominant modes are determined by the longest junction dimension in direction perpendicular to the applied magnetic field. Here we present measurements that emphasize the influence of Fiske modes on detector resolution, maximum count rate and effective area.

2. Detector characterization

We are developing STJ detectors based on Nb–Al–AlOx–Al–Nb thin film technology. The devices discussed here consist of a 265 nm Nb base electrode, an Al–AlOx–Al tunnel junction with 50 nm thick Al layers that serve as quasiparticle traps [17], and a 165 nm top Nb absorber. Device areas range from 70 μm × 70 μm to 200 μm × 200 μm. The devices are fabricated at Conductus Inc. using a modified photolithographic trilayer process [18]. The STJ detectors are operated in a single-stage adiabatic demagnetization refrigerator (ADR) with a base temperature of 60 mK and a hold time of 4–8 h below 0.4 K. The ADR temperature is not regulated as the device response is temperature independent below 0.4 K. A magnetic field of 100 G is applied in the plane of the junction in direction of the junction diagonal to suppress the DC Josephson current and reduce the magnitude of Fiske mode resonances [16]. The detectors face a port in the side of the ADR that can be attached to an X-ray fluorescence source or a synchrotron beam line. The detector response is read out with a current-sensitive pre-amplifier whose DC voltage bias allows stable biasing between Fiske modes and in regions of negative dynamic resistance [19]. The pulses are processed with a commercial Canberra 2020 shaping amplifier and captured with a Nucleus pulse height analyzer. For details of the experimental setup see Refs. [6,14].

2.1. Bias dependence

Fig. 1 shows the response of a 70 μm × 70 μm STJ detector to 70 eV photons as a function of STJ bias voltage, measured at a temperature of 250 mK and a magnetic field of 80 G. The data were taken in direct illumination at beam line 8-1 at the Stanford Synchrotron Radiation Laboratory (SSRL). The detector dark current (bottom trace) follows roughly an exponential function, characteristic of SIN tunneling in regions of trapped flux. In addition, a small residual DC Josephson current at low voltage and three Fiske mode resonances are visible at voltages of 160, 330 and 460 μV. A fourth Fiske mode resonance at a voltage of 220 μV is completely suppressed at this magnetic field. While

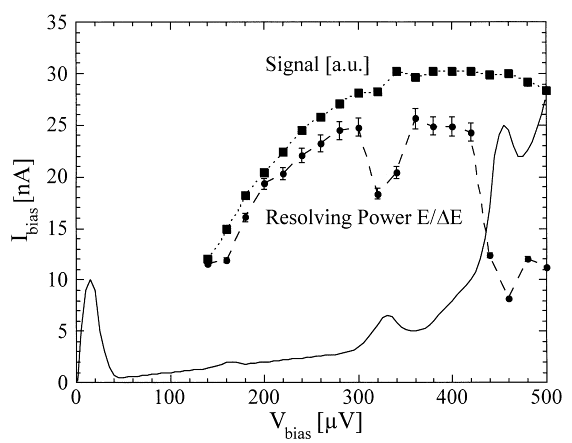

Fig. 1. Peak current signal (squares) and resolving power E/ΔE (circles) as a function of bias voltage for 70 eV photons. Note the drop in resolving power at Fiske mode resonances in the $I(V)$ characteristics (solid line).

it is possible to choose a magnetic field at which any one particular Fiske mode is reduced to zero, it is not possible to suppress all of them simultaneously for any magnetic field.

The signal magnitude (squares) is found to vary smoothly with bias voltage. It decreases at low bias when quasiparticles in the counterelectrode directly backtunnel into the absorber electrode before scattering inelastically, thereby canceling part of the signal. For bias voltages above 300 μV, i.e. when quasiparticles tunnel into the counterelectrode at least 300 μeV above the gap, the average scattering time is much faster than the tunneling time. Quasiparticles are then trapped in the counterelectrode by scattering before they can directly backtunnel and the full charge is collected [20]. Above 460 μV, the dynamic resistance of the detector becomes comparable to the effective input impedance of the pre-amplifier (~400 Ω), and thus part of the signal is lost through the device to ground.

The overall change in resolving power $E/\Delta E$ (circles) with bias follows the signal magnitude. At the optimum bias point, the resolution is 2.3 ± 0.1 eV FWHM and is limited by electronic noise. The resolving power decreases at low and very high bias where the signal magnitude drops while the electronic noise remains constant. In addition, at every Fiske mode, the resolution drops although the signal magnitude is unchanged. To verify that this drop is not due solely to a decrease in the STJ's dynamic resistance and thus an increased voltage noise contribution, we have biased the STJ on top of a Fiske mode where the dynamic resistance is infinite and still observe a dramatic decrease in resolving power.

Fig. 1 illustrates the influence of Fiske modes on the energy resolution in STJ detectors. For larger detectors, Fiske modes become more closely spaced in voltage. Eventually, they overlap and thereby preclude high-resolution operation. It is the interaction with Fiske modes rather than the increased device capacitance which first limits the maximum size of an individual high-resolution STJ detector.

2.2. Count rate

The response of the same detector was measured at SSRL beam line 1-1 using direct illumination with 277 eV photons corresponding to the carbon K line. By moving the detector in and out of the focal spot of the beam, the count rate was varied from 1000 to 55 000 counts/s (Fig. 2). No pile-up rejection was used in these measurements, and the stated output count rate reflects the dead time of the pulse height analyzer. At low count rates below 10 000 counts/s, the resolution at a bias voltage of 300 μV is 6.4 ± 0.3 eV FWHM at 277 eV (solid circles) and 11.2 ± 0.4 eV FWHM at the second-order energy of 554 eV (solid squares). Above 10 000 counts/s, pile-up starts to reduce the resolution. At a rate of 20 000 counts/s, the resolution is still 8.2 at 277 eV and 13.3 at 554 eV. These results are somewhat better than in earlier experiments [14], possibly because the present pre-amplifier is DC coupled to the detector, thus allowing the removal of the large coupling capacitor (1 μF) with its associated large discharge time constant. In these measurements, the source line width contributes about 2.9 eV to the resolution at 277 and 7.1 eV at 554 eV, because the monochromator's entrance and exit slits have to be opened to 100 μm for high photon flux. For 20 μm slits, the low count rate resolution improves to 5.7 ± 0.2 eV at 277 eV (open circles) and 8.7 ± 0.7 eV at 554 eV (open squares).

It is interesting to note that the maximum achievable count rate depends on the bias voltage.

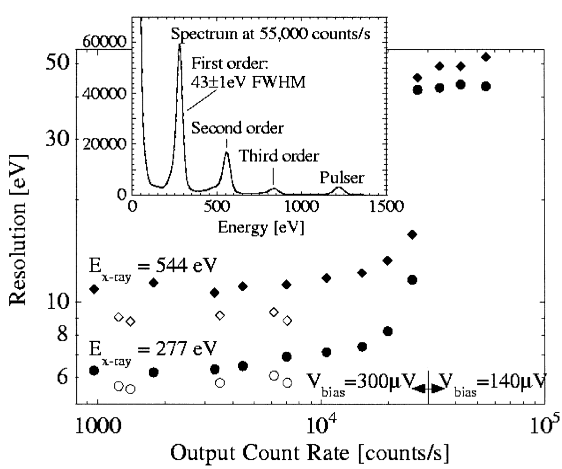

Fig. 2. Resolution at 277 eV (circles) and at 554 eV (squares) as a function of output count rate. The solid symbols are data taken with 100 μm × 100 μm monochromator slits and the open symbols are data for 20 μm × 20 μm slits.

Under the operating conditions discussed above, this particular device becomes unstable at count rates above 30 000 counts/s when biased at 300 μV. The response becomes chaotic, and no spectral information can be obtained. We believe that this instability arises from interference between the bias point and the pre-amplifier with the nearby Fiske modes, since stable operation at higher count rate is possible at a bias voltage of 140 μV below the lowest Fiske mode. At that bias, the lines are still clearly resolved, even at an output count rate of 55 000 counts/s (89 000 counts/s input count rate), albeit at a reduced resolution of 43 ± 1 eV (inset Fig. 2). This illustrates that Fiske modes can also limit the maximum count rate at which detectors can be operated at optimum resolution. There is no fundamental reason that tunnel junctions should become unstable above 30 000 counts/s, because stable operation at higher count rates and bias voltages above Fiske modes has been demonstrated [14]. Rather, the instability probably depends on the magnitude of the Fiske mode above the background current and the shift of the bias point during a pulse, which makes it sensitively dependent on operating temperature, magnetic field, bias voltage, device size and pre-amplifier type.

2.3. Device size

Fiske modes also impose limitations on the maximum device size of a single STJ detector, because in large devices the number of Fiske modes increases until they overlap and make it impossible to find a bias point that is not affected by at least one of them. We have addressed this problem by operating four 200 μm × 200 μm STJs in parallel and reading them out with a single pre-amplifier. In this configuration, the position of the Fiske modes is still determined by the largest dimension of an *individual* junction, while the effective area is increased by a factor of four without any multiplexing. The trade-off lies in a reduced resolution, because a slightly different junction response cannot be corrected during calibration if all STJs are read out with the same amplifier. Fig. 3 shows two fluorescence spectra of MnO, one with a single 200 μm × 200 μm STJ (dashed line), and one with four of them in parallel (solid line). The operating

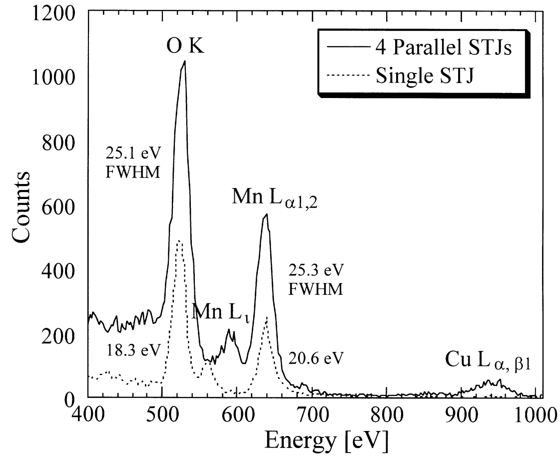

Fig. 3. Fluorescence spectra of MnO, one taken with a single 200 μm × 200 μm STJ (dotted line), one with four 200 μm × 200 μm STJs in parallel (solid line).

conditions are optimized for four-junction operation. The increased number of counts in the larger device is clearly visible. The shift of the Mn L_ι line is not yet understood. Under conditions optimized for single junction operation, this same junction shows a resolution of 10.4 eV at oxygen K. The resolution of 25 eV for the four combined devices indicates that the junction response varies by a few percent over distances of 1 mm on a chip. Operating several junctions in parallel is a simple way to increase the detector area with only moderate loss in resolution. Improved device uniformity and SQUID readout may allow operating many more STJs simultaneously for low count rate applications where large detector area is more important than highest resolution.

3. Summary

We have studied the influence of Fiske mode resonances on the performance of Nb-based STJ detectors. The best energy resolution of 2.3 eV FWHM at 70 eV at low count rate and 8.2 eV FWHM at 277 eV at a count rate of 20 000 counts/s is achieved when the detector is biased far away from Fiske modes. Biasing near Fiske modes reduces the detector resolution, and can also limit the maximum count rate. Furthermore, Fiske modes limit the maximum area of an individual STJ detector, as Fiske modes are more closely spaced in bias voltage in larger detectors. This problem can be addressed by operating several individual junctions in parallel with a single pre-amplifier, although this increase in area comes at the expense of reduced energy resolution due to the different response of each individual junction. In future devices, Fiske modes may be avoided altogether by developing STJ detectors with magnetic tunneling barriers.

Acknowledgements

We thank Jan Batteux and Jeff Moore for expert technical assistance. This work was performed under the auspices of the US Department of Energy by LLNL under contract no. W-7405-ENG-48 at the Stanford Synchrotron Radiation Laboratory (SSRL) which is operated by the DOE, Office of Basic Energy Sciences. Funding for this research was provided by the DOE, Office of Biological and Environmental Research, by the NIH through grant no. GM 44380, and by NASA through SBIR Contract no. NAS5-32805 and through UV detector development grant no. NAG5-4137.

References

[1] N.E. Booth, D.J. Goldie, Supercond. Sci. Technol. 9 (1996) 493.
[2] D. Twerenbold, Rep. Prog. Phys. 59 (1996) 349.
[3] H. Kraus, F.V. Freilitzsch, J. Jochum, R.L. Mößbauer, T. Peterreins, F. Pröbst, Phys. Lett. B 231 (1989) 195.
[4] D. McCammon, W. Cui, M. Juda, J. Morgenthaler, J. Zhang, R.L. Kelley, S.S. Holt, G.M. Madejski, S.H. Moseley, A.E. Szymkowiak, Nucl. Instr. and Meth. A 326 (1993) 157.
[5] D.A. Wollman, K.D. Irwin, G.C. Hilton, L.L. Dulcie, D.E. Newbury, J.M. Martinis, J. Microsc. 188 (1997) 196.
[6] M. Frank, C.A. Mears, S.E. Labov, L.J. Hiller, J.B. LeGrand, M.A. Lindeman, H. Netel, D. Chow, A.T. Barfknecht, J. Synchrotron Rad. 5 (1998) 515.
[7] W.H. Benner, D.M. Horn, J.M. Jaklevic, M. Frank, C.A. Mears, S.E. Labov, A.T. Barfknecht, J. Am. Soc. Mass Spectrom. 8 (1997) 1094.
[8] S. Friedrich, L.J. Hiller, M. Frank, J.B. le Grand, C.A. Mears, B. Nideröst, S.E. Labov, A.T. Barfknecht, M. LeGros, S.P. Cramer, J. Electron Spectr. Relat Phenomena 101 (1999) 891.
[9] E. Silver, M. LeGros, N. Madden, J. Beeman, E. Haller, X-ray Spectrom. 25 (1996) 115.
[10] A. Alessandrello, J.W. Beeman, C. Brofferio, O. Cremonesi, E. Fiorini, A. Giuliani, E.E. Haller, A. Monfardini, A. Nuciotti, M. Pavan, G. Pessina, E. Previtali, L. Zanotti, Phys. Rev. Lett. 82 (1999) 513.
[11] P. Hettl, G. Angloher, F.V. Freilitzsch, J. Höhne, J. Jochum, H. Kraus, R.L. Mößbauer, Proceedings of the EDXRF Conference 1998 Bologna, in press.
[12] P. Verhoeve, N. Rando, A. Peacock, A. van Dordrecht, B.G. Taylor, D.J. Goldie, Appl. Phys. Lett. 72 (1998) 3359.
[13] J.B. LeGrand, C.A. Mears, L.J. Hiller, M. Frank, S.E. Labov, H. Netel, D. Chow, S. Friedrich, M.A. Lindeman, A.T. Barfknecht, Appl. Phys. Lett. 73 (1998) 1295.
[14] M. Frank, L.J. Hiller, J.B. LeGrand, C.A. Mears, S.E. Labov, M.A. Lindeman, H. Netel, D. Chow, A.T. Barfknecht, Rev. Sci. Instrum. 69 (1998) 25.
[15] M.D. Fiske, Rev. Mod. Phys. 36 (1964) 221.
[16] R.E. Eck, D.J. Scalapino, B.N. Taylor, Proceedings of the Ninth International Conference on Low Temperature Physics, in: J.G. Daunt (Ed.), Plenum, New York, 1964.
[17] N.E. Booth, Appl. Phys. Lett. 50 (1987) 293.
[18] A.T. Barfknecht, R.C. Ruby, H. Ko, IEEE Trans. Magn. 27 (1991) 970.
[19] S. Friedrich, K. Segall, M.C. Gaidis, C.M. Wilson, D.E. Prober, P.J. Kindlmann, A.E. Szymkowiak, S.H. Moseley, IEEE Trans. Appl. Supercond. 7 (1997) 3383.
[20] S. Friedrich, K. Segall, M.C. Gaidis, C.M. Wilson, D.E. Prober, A.E. Szymkowiak, S.H. Moseley, Appl. Phys. Lett. 71 (1997) 3901.